PERGAMON

International Journal of Heat and Mass Transfer 42 (1999) 263–273

International Journal of HEAT and MASS TRANSFER

The combined effects of wall longitudinal heat conduction, inlet fluid flow nonuniformity and temperature nonuniformity in compact tube–fin heat exchangers: a finite element method

Ch. Ranganayakulu[a,*], K. N. Seetharamu[b]

[a]*Aeronautical Development Agency, P.B. No. 1718, Vimanapura Post, Bangalore, 560 017, India*
[b]*Department of Mechanical Engineering, Indian Institute of Technology, Madras, 600 036, India*

Received 20 November 1996; in final form 19 March 1998

Abstract

A finite element analysis of a crossflow tube–fin compact heat exchanger is presented. The analysis takes into account the combined effects of one-dimensional longitudinal heat conduction through the exchanger wall and nonuniform inlet fluid flow and temperature distributions on both hot and cold fluid sides. A mathematical equation is developed to generate different types of fluid flow/temperature maldistribution models considering the possible deviations in fluid flow. Using these fluid flow/temperature maldistribution models, the exchanger effectiveness and its deterioration due to the combined effects of longitudinal heat conduction and flow/temperature nonuniformity are calculated for various design and operating conditions of the exchanger. It was found that the performance deteriorations are quite significant in some typical applications due to the combined effects of longitudinal heat conduction, temperature nonuniformity and fluid flow nonuniformity on crossflow tube–fin heat exchanger.

Nomenclature

a elemental length of the exchanger in the x-direction [m]
A total heat transfer area [m^2]
A_W total solid elemental area available for longitudinal heat conduction [m]
b elemental length of the exchanger in the y-direction [m]
c_p specific heat of the fluid at constant pressure [J kg^{-1} K^{-1}]
C $(=mc_p)$ fluid heat capacity rate [W K^{-1}]
D pressure gradient constant in equation (4)
FN flow nonuniformity case
h convection heat transfer coefficient [W m^{-2} K^{-1}]
I divisions in the x-direction $(1, 2, 3, \ldots, n)$
J divisions in the y-direction $(1, 2, 3, \ldots, n)$
k thermal conductivity of the exchanger wall [W m^{-1} K^{-1}]
L, l the length of the elemental exchanger in x- and y-directions, respectively [m]
LHC longitudinal heat conduction case
m mass flow rate [kg s^{-1}]
NTU number of transfer units, AU/C_{min}, dimensionless
Q enthalpy/heat entering or leaving the plate [W]
P exchanger tube perimeter [m]
q enthalpy/heat entering/leaving the plate per unit area [W m^{-2}]
T temperature [°C]
TN temperature nonuniformity case
U overall heat transfer coefficient [W m^{-2} K^{-1}]
x flow length along hot fluid [m]
y flow length along cold fluid [m].

Greek symbols

α flow nonuniformity parameter as defined in equation (5)
λ longitudinal heat conduction parameter as defined in equation (15), dimensionless
ε_0 exchanger effectiveness without longitudinal conduction and flow nonuniformity, dimensionless

* Corresponding author. E-mail: rangan@ada.ernet.in.

0017–9310/98 $19.00
PII: S0017-9310(98)00156-2

$\varepsilon_{LHC,FN,TN}$ exchanger effectiveness with longitudinal heat conduction, temperature nonuniformity and flow nonuniformity, dimensionless
η overall extended surface efficiency, dimensionless
τ conduction effect factor as defined in equation (16), dimensionless.

Subscripts
c cold side
b bottom plate
h hot side
i inlet
m middle plate
max maximum magnitude
min minimum magnitude
o outlet
t top plate
w metal wall and 1–6 node numbers when used with T.

1. Introduction

The demand for high performance heat exchange devices having small spatial dimensions is increasing due to their need in applications such as aerospace and automobile applications, cooling of electronic equipment and artificial organs. The accurate prediction of the thermal performance of a compact heat exchanger in the design stage is highly desirable for most aerospace applications. In a heat exchanger, due to heat transfer taking place, temperature gradients exit in both fluids and in the separating wall, in the fluid flow directions. In most heat transfer and pressure drop calculations of heat exchangers, it is presumed that the inlet flow and temperature distributions across the exchanger core are uniform. These assumptions are generally not realistic under actual operating conditions due to various reasons. Advancement of the heat exchanger design theory, which takes these effects into consideration, therefore becomes an important project in industry.

The longitudinal heat conduction (LHC) through the heat exchanger wall structure in the direction of fluid flows has the effect of decreasing the exchanger performance for a specified NTU, and this reduction may be quite serious in exchangers with short flow length designed for high effectiveness ($>80\%$) [1]. These effects have been well recognized and the numerical data are available in [2, 3] for periodic-flow heat exchangers and in [4–6] for the direct transfer type heat exchangers.

The flow maldistribution effects have been well recognized for heat exchangers. The flow nonuniformity through the exchanger is generally associated with improper exchanger entrance configuration, due to poor header design and imperfect passage-to-passage flow distribution in a highly compact heat exchanger caused by various manufacturing tolerances. The flow nonuniformity (FN) effects have been well recognized and presented for heat exchangers [7–12]. Similarly, the fluid inlet temperature nonuniformity (TN) effects have also been investigated for crossflow heat exchangers [13, 14]. Investigation of the deterioration of exchanger performance due to two-dimensional flow nonuniformity on both fluid sides is very limited [7, 11].

In actual practice, heat exchangers may be subjected to wall LHC, inlet FN and TN together. No literature is available on the investigation of combined effects of LHC, TN and FN for a crossflow tube–fin heat exchanger. Generally, the wall LHC effect in a tube–fin heat exchanger is one-dimensional. Moreover, all the previous works [8–11] were limited to specific types of nonuniform flow models and cannot be interpolated or extrapolated for other types of flow maldistributions. No generalized solutions are available for interpolation/extrapolation of results for possible FN or TN, due to inlet poor header design, along with exchanger wall LHC effects. In this paper, the combined effects of LHC, TN and FN using a finite element method are presented and discussed for a crossflow tube–fin compact heat exchanger. The design of the headers and inlet ducts significantly affects the velocity distribution approaching the face of the exchanger core as shown in Fig. 1(a). In this type of FN, the variations in the fluid flow at the inlet of the exchanger core mainly depend on the location of the inlet duct, the ratio of core frontal area to inlet duct cross-sectional area, the distance of transition duct/header between the core face and inlet duct and the shape of headers, i.e. oblique flow headers or normal flow headers and with/without manifolds. In these cases, generally, the pressure gradient is often higher at the centre than that at the edge of the exchanger core.

2. Mathematical equations

Based on the concept of Fourier series a mathematical equation is developed to generate the flow nonuniformity models at exchanger inlet (either hot fluid side or cold fluid side) duct. The heat exchanger core frontal face is a rectangular domain having edges $2a$, $2b$ in x–y plane as shown in Fig. 1(b) and will be a square domain when $a = b$. The lengths with respect to origin 'o' are $x = a$ or $x = -a$ and $y = b$ or $y = -b$. The cold or hot fluid flows under the influence of a constant pressure gradient and its equation can be represented here:

$$\frac{\partial^2 W}{\partial x^2} + \frac{\partial^2 W}{\partial y^2} = \frac{1}{\mu}\frac{\partial P}{\partial z}. \tag{1}$$

On the boundary,

$$\text{at } x = \pm a, \quad W(\pm a, y) = 0 \tag{2}$$

$$\text{at } y = \pm b, \quad W(x, \pm b) = 0. \tag{3}$$

The term $(1/\mu)(\partial P/\partial z)$ is a constant that can be

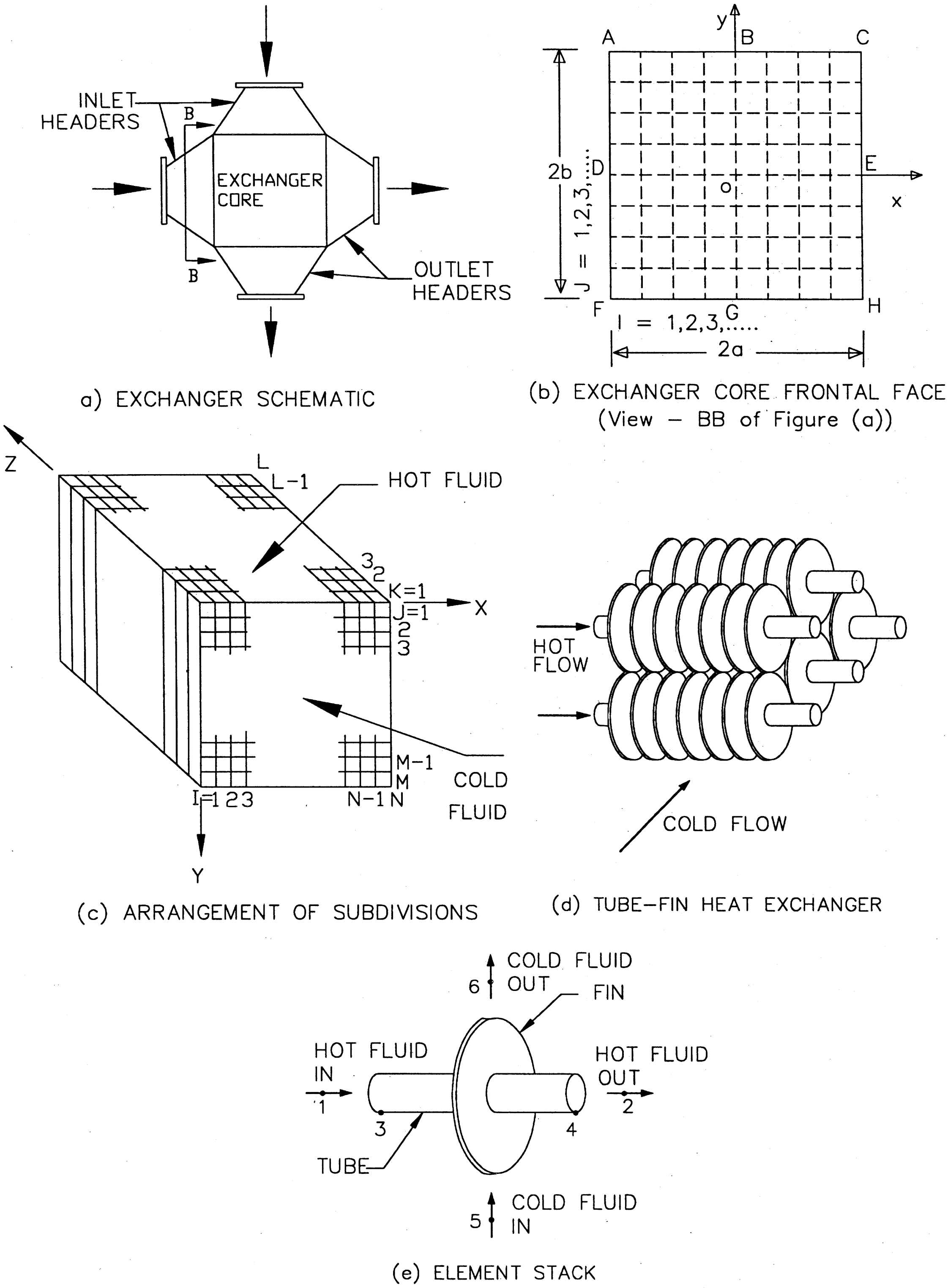

Fig. 1. (a) Exchanger schematic, (b) exchanger core frontal face, (c) arrangement of divisions, (d) tube–fin heat exchanger and (e) an element.

regarded as known since the choice of the pressure gradient is in one's control here. As such there is only one unknown, viz $W = W(x, y)$, controlled by equations (1)–(3) above. The solution to represent the fluid velocity (W) is

$$W(x,y) = \frac{64D}{\Pi^4} \sum_{m,n=0}^{\infty} \left\{ \frac{(-1)^{m+n+1}}{\left(\frac{2m+1}{a}\right)^2 + \left(\frac{2n+1}{b}\right)^2} \frac{\cos\frac{(2m+1)\Pi x}{2a} \cos\frac{(2n+1)\Pi y}{2b}}{(2m+1)(2n+1)} \right\}. \quad (4)$$

The local inlet flow/temperature nonuniformity parameter (α) is defined as [8],

$$\alpha = \frac{\text{actual inlet fluid flow/temperature}}{\text{average inlet flow/temperature}} . \quad (5)$$

if flow/temperature distribution is uniform

Consider that the fluid (either cold or hot) flowing in the y-direction is not uniformly distributed over the exchanger core on the x–z plane. Similarly, the fluid (either hot or cold) flowing in the x-direction is not uniformly distributed over the exchanger core on the y–z plane. The actual flow field within each compartment of the heat exchanger is very complex for both the hot and cold fluid sides. In fact, the fluid velocity will be zero at the walls of each compartment and will have a peak value in the middle. However, the peak velocity value itself varies from compartment to compartment, i.e., small value in the corner regions and a large value in the central portion, thus causing flow nonuniformity over the heat exchanger cross-section. In the present analysis, instead of the actual velocity field through each compartment, an average value has been taken for the whole compartment. This average value is assumed to be the same as given by the mean velocity over the compartment for the fully developed profile (laminar or turbulent) over the whole heat exchanger cross-section. In general, equation (4) can be used only to generate one type of nondimensional flow nonuniformity model at the entry of the exchanger duct. Using the above equation, different types of flow/temperature nonuniformity models are generated by distorting the velocity profile and keeping the average mass flow rate as unity. These models, named as A0, A1 and A5 depending on its magnitude of nondimensional parameter (α), are tabulated in Table 1. Also, the inlet flow nonuniformity for a typical flow/temperature model A0 having the highest magnitude of maldistribution is shown in Fig. 2. The velocity at the wall of the inlet duct is zero. The non-zero velocity values in the proposed models are at the points away from the wall of the transition duct. In each model, there are 10×10 local flow nonuniformity dimensionless parameters (α's), which correspond to the 10×10 subdivisions on the x–z plane perpendicular to the direction of nonuniform fluid flow/temperature. In view of the symmetry of the equation (4) with respect to o–x and o–y, only one-fourth of flow/temperature nonuniformity parameters (αs) are presented in Table 1.

Table 1
Flow/temperature nonuniformity parameters (αs)

$I =$	1; 10	2; 9	3; 8	4; 7	5; 6
Model A0					
$J =$ 1; 10	0.100	0.100	0.100	0.100	0.100
2; 9	0.100	0.352	0.597	0.819	0.996
3; 8	0.100	0.597	1.080	1.523	1.879
4; 7	0.100	0.819	1.523	2.177	2.717
5; 6	0.100	0.996	1.879	2.717	3.438
Model A1					
$J =$ 1; 10	0.500	0.500	0.500	0.500	0.500
2; 9	0.500	0.639	0.776	0.899	0.998
3; 8	0.500	0.776	1.045	1.291	1.489
4; 7	0.500	0.899	1.291	1.655	1.956
5; 6	0.500	0.998	1.489	1.956	2.356
Model A5					
$J =$ 1; 10	0.900	0.900	0.900	0.900	0.900
2; 9	0.900	0.923	0.952	0.978	0.999
3; 8	0.900	0.952	1.009	1.062	1.104
4; 7	0.900	0.978	1.062	1.139	1.203
5; 6	0.900	0.999	1.104	1.203	1.289

3. Finite element method

The arrangement of subdivisions is shown in Fig. 1(c). A model of a tube–fin heat exchanger is shown in Fig. 1(d). It is divided into a number of elements. This is an element which carries hot and cold fluids as shown in Fig. 1(e). Since, the wall temperature distribution in a crossflow tube–fin heat exchanger is one-dimensional, a two-noded element has been considered for studying the one-dimensional LHC effects on tube wall. These are the basic elemental exchangers for which the finite element equations are formulated as coupled conduction–convection problems [16]. The linear elements (2-noded) for both hot and cold fluids are considered in the present analysis. The following assumptions are made in this analysis:

(1) Thickness of the exchanger wall is small when compared with its other two dimensions, so that the thermal resistance through the exchanger wall in the direction normal to the fluid flows is small enough to be neglected.
(2) There is no phase change and no heat generation within the exchanger.

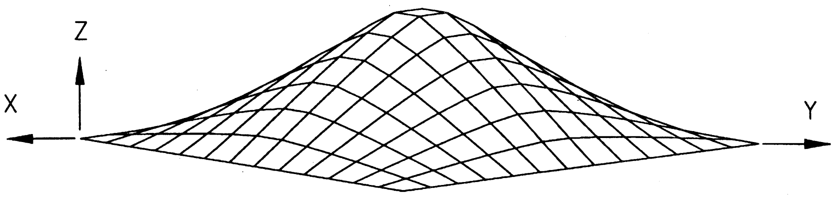

Fig. 2. Flow nonuniformity model A0.

(3) Fluids other than liquid metals are considered.
(4) Both fluids within the exchanger are considered unmixed. Cross or transverse mixing of fluids is not considered.
(5) The heat transfer surface configurations and the heat transfer areas on both sides per unit base area are constant and uniform throughout the exchanger.
(6) The entry length effects are not considered in the present analysis.
(7) Steady state conditions are assumed.

Based on the above assumptions, the governing energy balance equations considering one-dimensional LHC on the exchanger are formulated as shown below:

$$-(MC_{\mathrm{p}})_{\mathrm{h}}\frac{\partial T_{\mathrm{h}}}{\partial x}+(\vartheta hP)_{\mathrm{h}}(T_{\mathrm{h}}-T_{\mathrm{w}})=0 \tag{6}$$

$$(kA_{\mathrm{w}})\frac{\partial^2 T_{\mathrm{w}}}{\partial x^2}+(\vartheta hP)_{\mathrm{h}}(T_{\mathrm{h}}-T_{\mathrm{w}})-(\vartheta hP)_{\mathrm{c}}(T_{\mathrm{w}}-T_{\mathrm{c}})=0 \tag{7}$$

$$(MC_{\mathrm{p}})_{\mathrm{c}}\frac{\partial T_{\mathrm{c}}}{\partial x}-(\vartheta hP)_{\mathrm{c}}(T_{\mathrm{w}}-T_{\mathrm{c}})=0. \tag{8}$$

The boundary conditions are,

$$T_{\mathrm{h}}(0,y)=T_{\mathrm{h,in}};\quad T_{\mathrm{c}}(x,0)=T_{\mathrm{c,in}}. \tag{9}$$

The temperature variation of the hot fluid (T_{h}), cold fluid (T_{c}) and the wall (T_{w}) in the element are approximately by a linear variation as

$$T_{\mathrm{h}}=N_iT_i+N_jT_j \tag{10}$$

$$T_{\mathrm{c}}=N_kT_k+N_lT_l \tag{11}$$

$$T_{\mathrm{w}}=N_iT_i+N_jT_j \tag{12}$$

where N_i, N_j, N_k and N_l are shape functions, $N_i=l-x/a$, $N_j=x/a$ for cold fluid and wall and $N_k=l-y/b$, $N_l=y/b$ for hot fluid.

The boundary conditions to be satisfied are

$$(\alpha MC_{\mathrm{p}})_{\mathrm{h}}T_1=Q_{\mathrm{h}} \tag{13}$$

$$(\alpha MC_{\mathrm{p}})_{\mathrm{c}}T_5=Q_{\mathrm{c}}. \tag{14}$$

The following dimensionless parameters are introduced to study the influence of LHC, TN and FN on the exchanger performance:

(a) LHC parameter $(\lambda)=(kA_{\mathrm{w}})/(LC_{\min})$ (15)

(b) Correction factor $(\tau)=\dfrac{\varepsilon_0-\varepsilon_{\mathrm{LHC,FN,TN}}}{\varepsilon_0}$. (16)

The correction factor (τ) directly shows the degree of performance variations of the exchanger effectiveness. Substituting the approximation in the above equations and using Galerkin method [17], the final set of element matrices are obtained as shown in Appendix A. In crossflow tube–fin heat exchanger, the wall temperature distribution is one-dimensional. A two-noded element has been taken for wall temperature distribution. Hence, a 6×6 element matrix has been obtained as shown in Appendix A. The element matrices for other pairs of the stacks are evaluated and assembled into a global matrix. The final set of simultaneous equations are solved after incorporating the known boundary conditions (inlet temperatures). Thus by marching in a proper sequence, the temperature distribution in the exchanger is obtained. The heat transfer surface geometry {CF-9.05-3/4 J(C)} for finned tube heat exchanger is taken from Kays and London [1]. The heat transfer coefficients are evaluated for above surface geometry using procedures given by Kays and London [1] at the bulk mean temperatures of the fluids. If the temperatures are not known a priori, the iteration is started with assumed outlet temperatures. The new outlet temperatures are calculated and compared with assumed outlet temperatures. The iterations are continued until the convergence is achieved to the fourth digit for all cases. Analytical solutions without considering the effects of LHC, TN and FN are obtained using the solution procedure given by Kays and London [1] and Shah [18]. In this study, the exchanger thermal performance deteriorations due to LHC, TN and FN are plotted as a function of NTU ($\mathrm{NTU}_{\mathrm{overall}}$) for three magnitudes of $C_{\min}/C_{\max}$ (1.0, 0.6 and 0.2) and for three magnitudes of λ (0.05, 0.1 and 0.2) for the following cases:

(a) the combined effects of LHC, TN and FN on $C_{\min}$ fluid side;
(b) the combined effects of LHC, TN and FN on $C_{\max}$ fluid side;
(c) the combined effects of LHC, TN and FN on both $C_{\min}$ and $C_{\max}$ fluid sides.

4. Comparison of results

The accuracy of the solution depends on the number of the elements used. Actually, the number of elements used is determined by a compromise between the accuracy desired and the time required by the computer. No information is available on the investigation of combined effects of LHC, TN and FN for crossflow tube–fin heat exchangers. However, the present finite element analysis has been validated with the individual effects of TN [13] and FN [8] of a crossflow plate–fin heat exchanger. The relative comparison with the present finite element results is shown in Fig. 3. This comparison is found to be good. The accuracy is believed to be sufficient for most of the engineering applications.

The complete analysis of individual effects of LHC, FN and TN for a tube–fin heat exchanger is available in [6, 12]. However, the individual effects of LHC, FN and TN of a tube–fin heat exchanger are compared with the combined effects of LHC, FN and TN and shown in Fig. 4 for ready reference. This figure indicates that the performance variation due to combined effect LHC, FN and TN is not just the cumulative sum of its individual effects. Hence the detailed analysis has been carried out for combined effects of LHC, FN and TN in a crossflow tube–fin heat exchanger.

Chiou [13] has studied the effects of inlet fluid temperature nonuniformity on the thermal performance of crossflow heat exchanger using specified temperature nonuniformity models. He has observed some significant augmentation in thermal performance of crossflow heat exchanger due to large variations in temperature differences between hot and cold fluids in the core. Similarly,

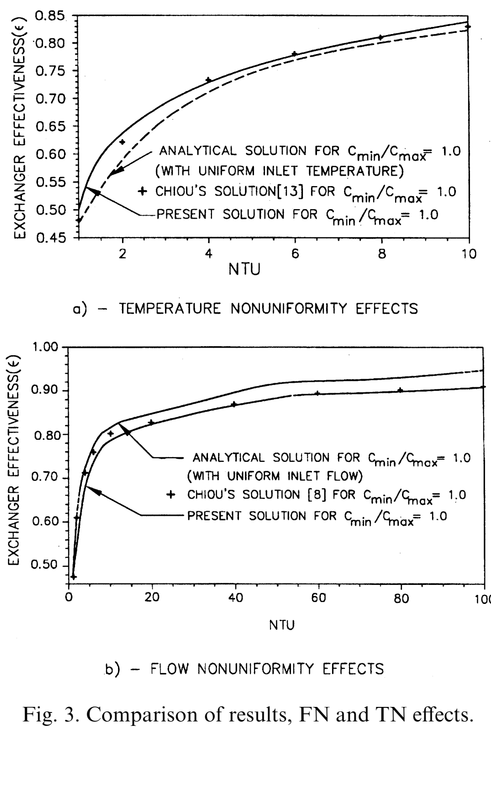

Fig. 3. Comparison of results, FN and TN effects.

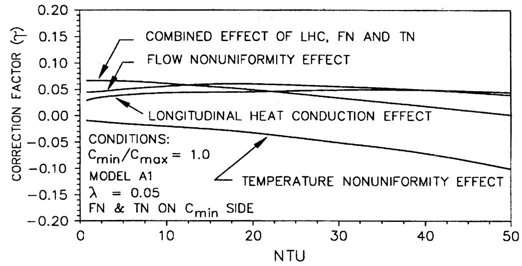

Fig. 4. Comparison of individual effects and combined effects of LHC, FN and TN.

the temperature nonuniformity effects have been shown in Fig. 5 by reversing the model A1 on C_{min} fluid side and C_{max} fluid side. It is observed that there is significant augmentation in performance when TN model A1 is considered on C_{max} fluid side. It is noted from this figure that the correction factor is positive up to NTU equal to six when the TN model is considered on C_{min} fluid side. This is due to heat transfer process because of large variations in temperature differences in the exchanger zone.

5. Results and discussion

In this analysis, air is used as cold and hot fluids and an unmixed–unmixed crossflow exchanger is considered. Heat exchanger surface geometry CF-9.05-3/4 J(C) from Kays and London [1] is used for estimation of heat transfer coefficients. In most cases, even a large variation in some physical properties of air are reflected only marginally in the performance variations as observed by other investigators [19, 20].

In this paper, the performance evaluation with the combined effects of wall LHC and inlet fluid FN and TN on a crossflow tube–fin heat exchanger is presented for balanced flow, $C_{min}/C_{max} = 1$, as well as for unbalanced

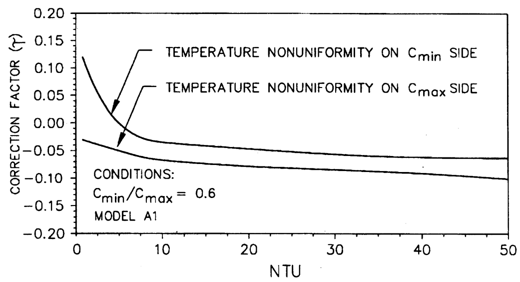

Fig. 5. Temperature nonuniformity effects, crossflow tube–fin heat exchanger.

flow, C_{min}/C_{max} equal to 0.6 and 0.2. Figures 6–13 shows the combined effects of longitudinal heat conduction, inlet temperature nonuniformity and flow nonuniformity in the crossflow tube–fin heat exchanger. In each case, there are three figures (a, b and c) considering $\lambda = 0.2$, 0.1 and 0.05. It can be seen from these figures that the correction factor (τ) decreases with increasing of NTU for all cases of balanced and unbalanced flows as shown in Figs 6–13. It is noted that there is a significant augmentation in thermal performance (upto 10%), when the NTU is high and λ is low as shown in Figs 8–12. This augmentation in performance is due to the large variations between hot and cold fluid temperatures as observed by earlier investigators [13, 14]. However, this augmentation in performance is negligible for lower NTU values even when λ is equal to 0.05. This observation indicates that the effects of LHC, FN and TN on the deterioration of exchanger performance tend to eliminate each other in the region of large NTU, but tend to augment each other in the region of small NTU at higher values of λ. It has been observed that the performance variations are higher when the flow/temperature models are considered on C_{min} side. Also, it has been observed that the performance deteriorations are more for balanced flows as compared to that of unbalanced flows.

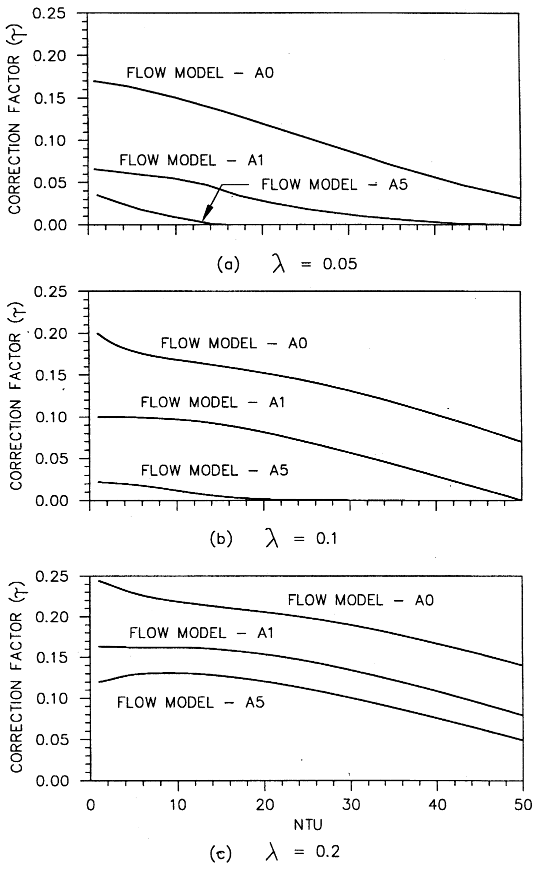

Fig. 6. Combined effects of longitudinal heat conduction, flow nonuniformity and temperature nonuniformity effects, tube–fin heat exchanger, C_{min} fluid side ($C_{min}/C_{max} = 1.0$).

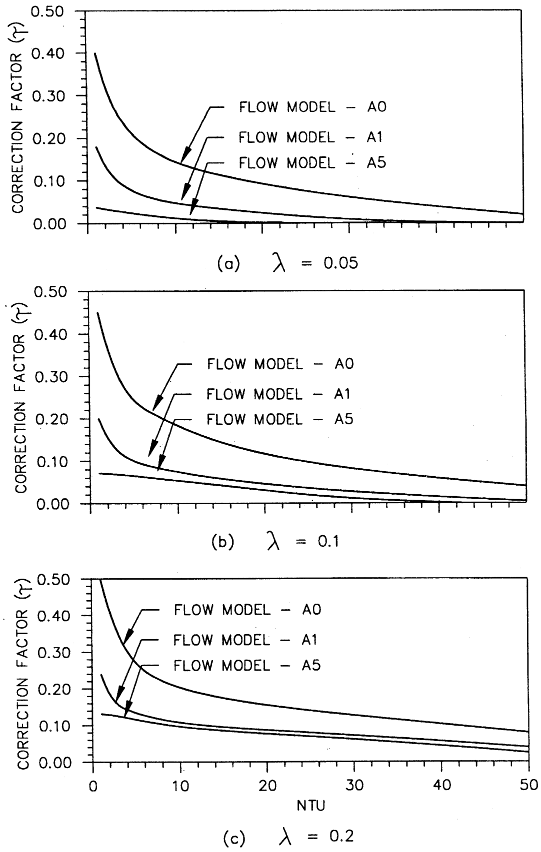

Fig. 7. Combined effects of longitudinal heat conduction, flow nonuniformity and temperature nonuniformity effects, tube–fin heat exchanger, both fluid side ($C_{min}/C_{max} = 1.0$).

The relative comparison of results are tabulated in Table 2. In this table, the combined effects of LHC, FN and TN are compared with individual effects of LHC, FN and TN for the crossflow tube–fin heat exchanger. The performance variations due to individual effects of LHC (at $\lambda = 0.05$), FN and TN at NTU = 10 for $C_{min}/C_{max} = 1.0$ for model A1 are 3.75, 5.95 and −2%, respectively, whereas the performance variation for the combined effects is around 6%. It can be seen from the table that the performance variations generally decrease when the LHC, TN and FN are considered together.

Information presented in these figures is not restricted to the models considered in this analysis, but the results can be interpolated for other similar flow models. For example, the results can be interpolated, for any inter-

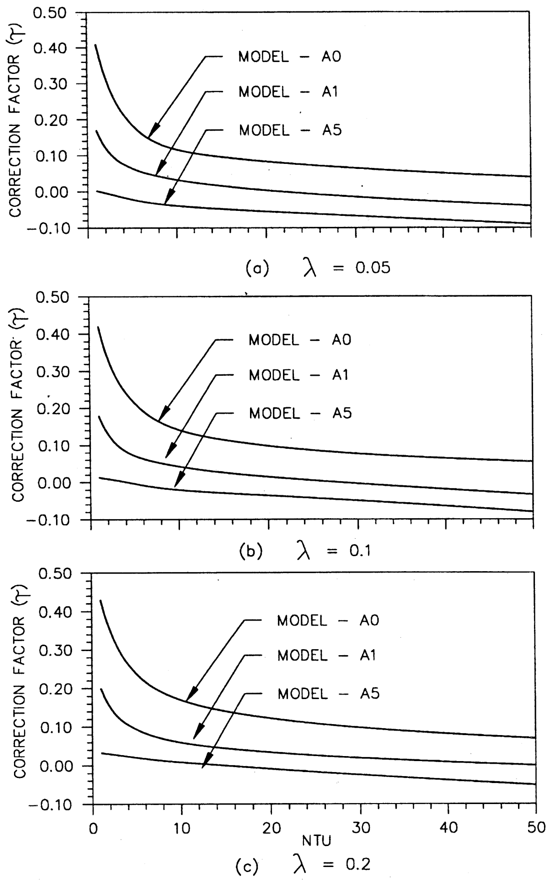

Fig. 8. Combined effects of longitudinal heat conduction, flow nonuniformity and temperature nonuniformity effects, tube–fin heat exchanger, C_{min} fluid side ($C_{min}/C_{max} = 0.6$).

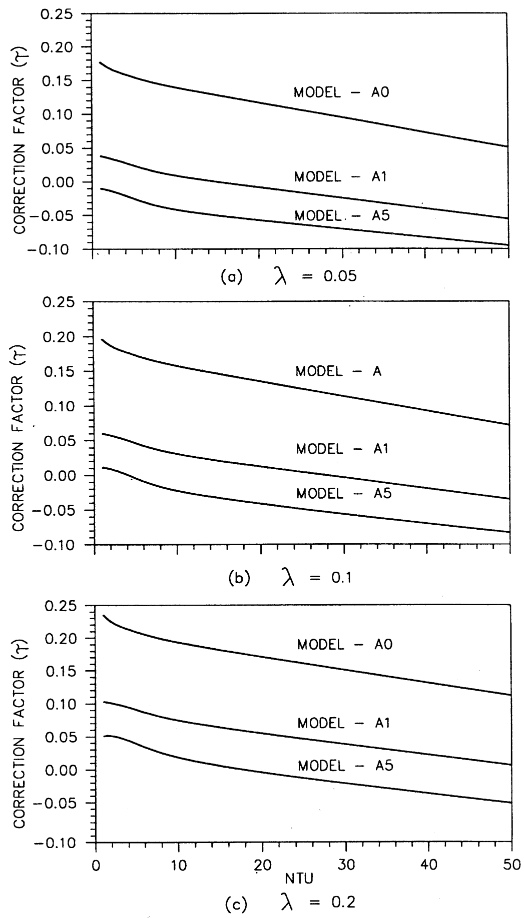

Fig. 9. Combined effects of longitudinal heat conduction, flow nonuniformity and temperature nonuniformity effects, tube–fin heat exchanger, C_{max} fluid side ($C_{min}/C_{max} = 0.6$).

Table 2
Effects of longitudinal wall heat conduction, flow and temperature nonuniformity crossflow tube–fin heat exchanger

Models	C^*	Performance variations (%)															
		NTU = 10								NTU = 50							
		LHC			FN	TN	LHC+FN+TN			LHC			FN	TN	LHC+FN+TN		
		$\lambda =$ 0.05	$\lambda =$ 0.1	$\lambda =$ 0.2			$\lambda =$ 0.05	$\lambda =$ 0.1	$\lambda =$ 0.2	$\lambda =$ 0.05	$\lambda =$ 0.1	$\lambda =$ 0.2			$\lambda =$ 0.05	$\lambda =$ 0.1	$\lambda =$ 0.2
A1	1.0	3.75	7.90	17.0	5.95	−2.0	6.00	9.90	14.0	4.00	17.5	5.00	4.95	−10.0	0.00	0.50	8.00
	0.6	1.85	3.50	7.50	2.25	−3.5	4.00	4.50	8.00	1.50	5.00	−4.0	1.80	−8.5	−4.00	−3.00	0.50
	0.2	0.60	0.85	1.00	1.20	−7.0	−5.0	−4.5	−4.0	0.00	0.00	−2.0	0.00	−3.0	−2.00	−1.75	−1.50
A5	1.0	3.75	7.90	17.0	0.15	−2.25	1.00	1.50	2.50	4.00	17.5	4.50	0.05	−11.0	−2.00	−1.00	5.00
	0.6	1.85	3.50	7.50	0.10	−5.0	−2.5	0.00	1.00	1.50	5.00	−5.0	0.00	−9.5	−8.00	−7.00	−5.00
	0.2	0.60	0.85	1.00	0.05	−7.5	−3.5	−3.0	−2.5	0.00	0.00	−2.5	0.00	−3.5	−2.25	−2.00	−1.75

Conditions: $C^* = C_{min}/C_{max}$, $(\vartheta hP)_h/(\vartheta hP)_c = 1.0$, and flow/temperature nonuniformity on the C_{min} fluid side.

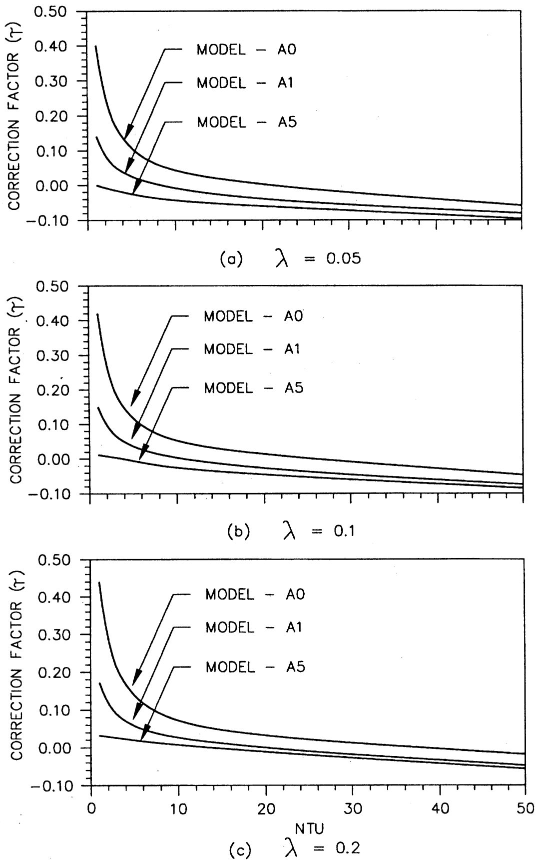

Fig. 10. Combined effects of longitudinal heat conduction, flow nonuniformity and temperature nonuniformity effects, tube–fin heat exchanger, both fluid side ($C_{min}/C_{max} = 0.6$).

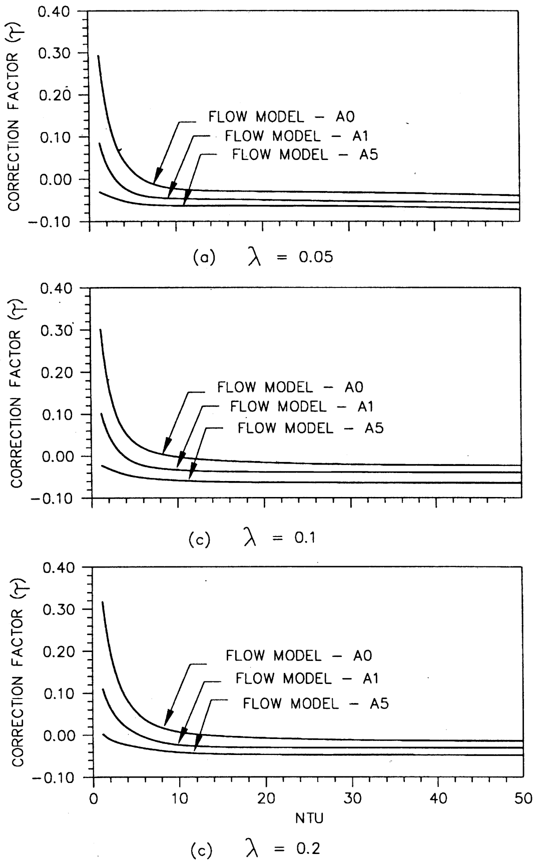

Fig. 11. Combined effects of longitudinal heat conduction, flow nonuniformity and temperature nonuniformity effects, tube–fin heat exchanger, C_{min} fluid side ($C_{min}/C_{max} = 0.2$).

mediate flow maldistribution model, between the curves, as the upper curve is showing higher performance deviations and lower curve is showing the minimum performance deviations. The deterioration in thermal performance of a single-pass crossflow tube–fin heat exchanger due to the combined effects of LHC, FN and TN presented in this section is generally similar to those reported in previous investigations [15] for crossflow plate–fin heat exchangers. However, the type of the fluid maldistributions considered in this investigation are basically different from those reported previously; direct comparison of all these results is thus not possible.

6. Conclusions

The performance variations of high-efficiency crossflow tube–fin compact heat exchangers are presented and evaluated for both balanced and unbalanced flows having the combined effects of wall longitudinal heat conduction, inlet fluid flow and temperature nonuniformity. A mathematical equation has been used to generate different types of fluid flow maldistribution models considering the possible deviations in fluid flow. The ranges of parameters investigated are: $1 \leqslant \mathrm{NTU} \leqslant 50$, $C_{min}/C_{max} = 1.0$, 0.6 and 0.2 and $\lambda = 0.05$, 0.1 and 0.2. The thermal performance variation of a crossflow compact tube–fin heat exchanger due to the combined effects wall longitudinal heat conduction, inlet flow/temperature nonuniformity is not always negligible, especially when the fluid capacity rate ratio of both fluids is equal to 1.0 and when the longitudinal heat conduction parameter (λ) is greater than 0.05. This estimation can reduce the number of tests and modifications of the prototype to a minimum for similar applications.

Acknowledgement

The authors wish to acknowledge their gratitude to the management of the Aeronautical Development Agency, Bangalore, for allowing publication of this paper.

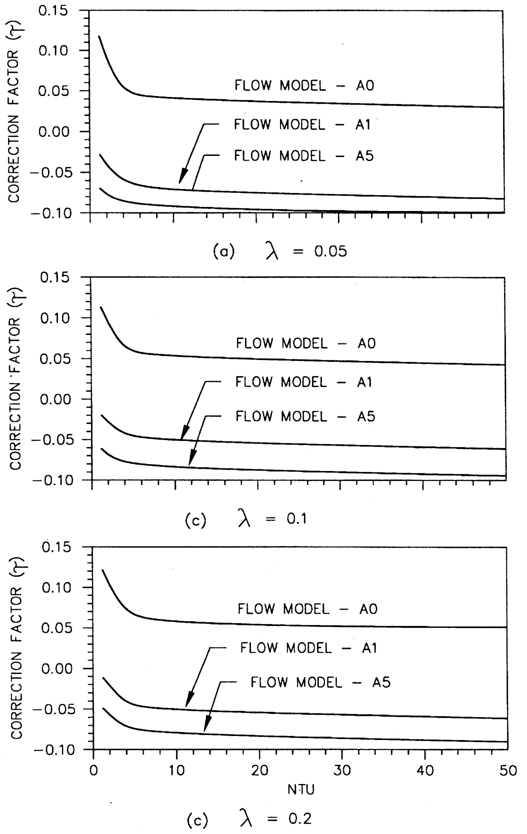

Fig. 12. Combined effects of longitudinal heat conduction, flow nonuniformity and temperature nonuniformity effects, tube–fin heat exchanger, C_{max} fluid side ($C_{min}/C_{max} = 0.2$).

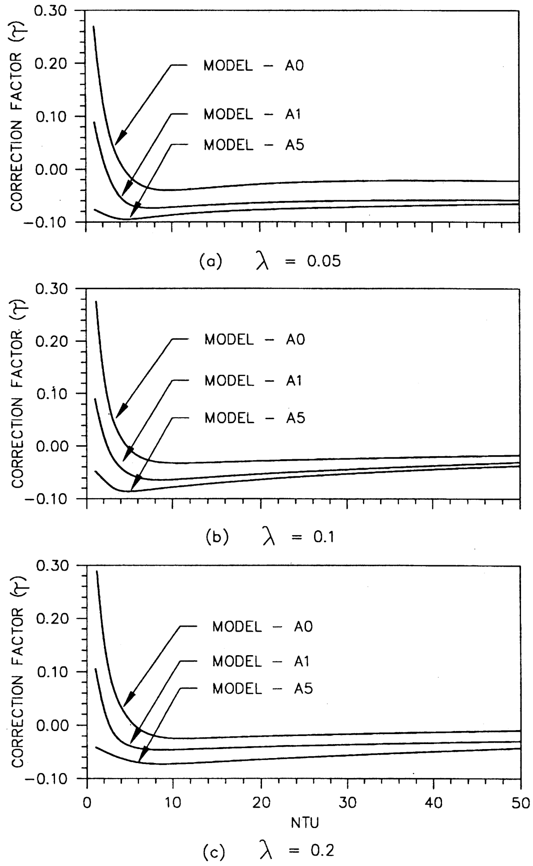

Fig. 13. Combined effects of longitudinal heat conduction, flow nonuniformity and temperature nonuniformity effects, tube–fin heat exchanger, both fluid side ($C_{min}/C_{max} = 0.2$).

Appendix A: crossflow tube–fin exchanger stack element

$$\begin{bmatrix} 2W_h & 0 & 0 & 0 & 0 & 0 \\ W_h+H_h & W_h+2H_h & -H_h & -2H_h & 0 & 0 \\ -2H_h & -H_h & K+2H_h+2H_c & K+H_h+H_c & -2H_c & -H_c \\ -H_h & -2H_h & -K+H_h+H_c & K+2H_h+2H_c & -H_c & -2H_c \\ 0 & 0 & 0 & 0 & -W_c & 0 \\ 0 & 0 & -H_c & -2H_c & -W_c+H_c & W_c+2H_c \end{bmatrix} \begin{bmatrix} T_1 \\ T_2 \\ T_3 \\ T_4 \\ T_5 \\ T_6 \end{bmatrix} = \begin{bmatrix} Q_h \\ 0 \\ 0 \\ 0 \\ Q_c \\ 0 \end{bmatrix}$$

where $K = kA_w/L$, $H = (\vartheta hPl)/6$, $W = \alpha(mC_p)/2$.

References

[1] W.M. Kays, A.L. London, Compact Heat Exchangers, 3rd ed., McGraw-Hill, New York, 1984.

[2] G.D. Bahnke, C.P. Howard, The effect of longitudinal heat conduction on periodic-flow heat exchanger performance, ASME J. Eng. for Power 86 (1964) 105–121.

[3] R.K. Shah, A correlation for longitudinal heat conduction effects in periodic-flow heat exchangers, ASME J. Eng. Power 97 (1975) 453–454.

[4] R.K. Shah, A review of longitudinal wall heat conduction in recuperators, J. Energy, Heat and Mass Transfer 16 (1994) 15–25.

[5] J.P. Chiou, The effect of longitudinal heat conduction on cross flow heat exchanger, ASME J. Heat Transfer 100 (1978) 46–351.

[6] Ch. Ranganayakulu, K.N. Seetharamu, K.V. Sreevatsan, The effects of longitudinal heat conduction in compact plate–fin and tube–fin heat exchangers using a finite element method, Int. J. Heat Mass Transfer 40 (6) (1997) 1261–1277.

[7] Ch. Ranganayakulu, K.N. Seetharamu, K.V. Sreevatsan, The effects of inlet fluid flow nonuniformity on thermal performance and pressure drops in crossflow plate–fin compact heat exchangers, Int. J. Heat Mass Transfer 40 (1) (1997) 27–38.

[8] J.P. Chiou, Thermal performance deterioration in a crossflow heat exchanger due to the flow nonuniformity, ASME J. Heat Transfer 100 (1978) 580–587.

[9] J.P. Chiou, The effect of air flow nonuniformity on the thermal performance of an automobile air conditioning condenser, SAE Trans., Paper No. 830542, 1984, pp. 2.587–2.600.

[10] J.P. Chiou, The effect of air flow nonuniformity on the thermal performance of an evaporator of automobile air conditioning system, SAE Trans., Paper No. 840381, 1985, pp. 2.991–2.1005.

[11] J.P. Chiou, Thermal performance deterioration in a crossflow heat exchanger due to the flow nonuniformity on both hot and cold sides, Proc. 6th Int. Heat Transfer Conference, Heat Transfer 4 (1978) 279–284.

[12] Ch. Ranganayakulu, K.N. Seetharamu, K.V. Sreevatsan, The performance evaluation of crossflow tube–fin heat exchanger considering the effects of inlet flow nonuniformity and temperature nonuniformity using a finite element method, in: R.W. Lewis et al. (Eds.), Proc. 9th Int. Conference on Numerical Methods in Thermal Problems, IX (2) (1995) 1010–1021.

[13] J.P. Chiou, The effect of nonuniformity of inlet fluid temperature on the thermal performance of crossflow heat exchanger, 7th Int. Heat Transfer Conference, Heat Transfer 1982, pp. 179–184.

[14] J.P. Chiou, The effect of nonuniform inlet air temperature distribution on the sizing of the engine radiator, SAE Trans., Paper No. 820078, 1982, pp. 250–260.

[15] J.P. Chiou, The advancement of compact heat exchanger theory considering the effects of longitudinal heat conduction and flow nonuniformity effects, in: R.K. Shah et al. (Eds.), Compact Heat Exchangers—History, Technological Advancement and Mechanical Design Problems, ASME, New York, Book No. G00183, HTD, 10 (1980) 101–121.

[16] J.H. Chin, D.R. Frank, Engineering finite element analysis of conduction, convection and radiation, in: R.W. Lewis (Ed.), Numerical Methods in Heat Transfer, vol. 3, John Wiley and Sons, 1984.

[17] L.J. Segerlind, Applied Finite Element Analysis, 2nd ed., John Wiley and Sons, 1982.

[18] R.K. Shah, Compact heat exchanger design procedures, in: S. Kakac, A.E. Bergles, F. Mayinger (Eds.), Heat Exchangers: Thermal-Hydraulic Fundamentals and Design, Hemisphere Publishing, New York, 1981, pp. 111–151.

[19] S.G. Ravikumar, K.N. Seetharamu, P.A. Aswatha Narayana, Performance evaluation of crossflow compact heat exchangers using finite elements, Int. J. Heat Mass Transfer 32 (1989) 889–894.

[20] H. Yamasheta, R. Izumi, S. Yamaguchi, Performance of crossflow heat exchangers with variable physical properties, Bulletin of JSME 20 (1977) 1008–1015.